THE JOURNAL OF BIOLOGICAL CHEMISTRY VOL. 286, NO. 2, pp. 1074–1082, January 14, 2011

Activated Inositol 1,4,5-Trisphosphate Receptors Are Modified by Homogeneous Lys-48- and Lys-63-linked Ubiquitin Chains, but Only Lys-48-linked Chains Are Required for Degradation*

Received for publication, September 24, 2010, and in revised form, November 1, 2010 Published, JBC Papers in Press, November 11, 2010, DOI 10.1074/jbc.M110.188383

Danielle A. Sliter[‡], **Mike Aguiar**[§], **Steven P. Gygi**[§], **and Richard J. H. Wojcikiewicz**[‡1]

From the [‡]*Department of Pharmacology, State University of New York Upstate Medical University, Syracuse, New York 13210 and the* [§]*Department of Cell Biology, Harvard Medical School, Boston, Massachusetts 02115*

Inositol 1,4,5-trisphosphate (IP_3) receptors (IP_3Rs) are large, ubiquitously expressed, endoplasmic reticulum membrane proteins that form tetrameric IP_3 and Ca^{2+}-gated Ca^{2+} channels. Endogenous IP_3Rs provide very appealing tools for studying the ubiquitin-proteasome pathway in intact mammalian cells because, upon activation, they are rapidly ubiquitinated and degraded. Using mass spectrometry, we previously examined the ubiquitination of IP_3R1 in αT3-1 pituitary gonadotrophs and found that IP_3R1 ubiquitination is highly complex, with receptors being modified at multiple sites by monoubiquitin and polyubiquitin chains formed through both Lys-48 and Lys-63 linkages (Sliter, D. A., Kubota, K., Kirkpatrick, D. S., Alzayady, K. J., Gygi, S. P., and Wojcikiewicz, R. J. H. (2008) *J. Biol. Chem.* 283, 35319–35328). Here, we have extended these studies to determine whether IP_3R2 and IP_3R3 are similarly modified and if ubiquitination is cell type-dependent. Using mass spectrometry and linkage-specific ubiquitin antibodies, we found that all IP_3R types are subject to ubiquitination at approximately the same locations and that, independent of cell type, IP_3Rs are modified by monoubiquitin and Lys-48- and Lys-63-linked ubiquitin chains, although in differing proportions. Remarkably, the attached Lys-48- and Lys-63-linked ubiquitin chains are homogeneous and are segregated to separate IP_3R subunits, and Lys-48-linked ubiquitin chains, but not Lys-63-linked chains, are required for IP_3R degradation. Together, these data provide unique insight into the complexities of ubiquitination of an endogenous ubiquitin-proteasome pathway substrate in unperturbed mammalian cells. Importantly, although Lys-48-linked ubiquitin chains appear to trigger proteasomal degradation, the presence of Lys-63-linked ubiquitin chains suggests that ubiquitination of IP_3Rs may have physiological consequences beyond signaling for degradation.

The ubiquitin-proteasome pathway (UPP)[2] is critical to cell homeostasis because it mediates the degradation of key proteins involved in fundamental cellular processes and allows for endoplasmic reticulum (ER)-associated degradation, a facet of the UPP that disposes of aberrant or unrequired proteins from the ER lumen and membrane (1, 2). Proteins targeted for degradation by the UPP are first ubiquitinated and then shuttled to the 26 S proteasome, a cytosolic protein complex that recognizes, unfolds, and degrades ubiquitinated substrates (3). Ubiquitination, the covalent attachment of the C-terminal glycine of ubiquitin to the ϵ-amino group of a lysine residue in a target protein, is typically mediated by the E1 ubiquitin-activating enzyme, the E2 ubiquitin-conjugating enzyme, and the E3 ubiquitin ligase (4). Repetition of this process can result in multiple monoubiquitination through attachment of additional ubiquitin moieties to different lysines within the target protein, or in the formation of ubiquitin chains through attachment of ubiquitin to any of seven lysines within ubiquitin itself (Lys-6, Lys-11, Lys-27, Lys-29, Lys-33, Lys-48, and Lys-63) or to the N-terminal methionine (5). The fate of a ubiquitinated protein is thought to be determined by the type of ubiquitin linkage associated with it. For example, it is generally accepted that proteins tagged with Lys-48-linked chains are targeted to the proteasome for degradation, whereas Lys-63-linked chains mediate a variety of events (*e.g.* the DNA damage response and protein trafficking) (6–8). However, this dogma is being challenged, for example, with new data indicating that ubiquitin chains utilizing lysines other than Lys-48 can contribute to proteasomal degradation (9–12). Ubiquitin can be removed from proteins through the action of deubiquitinating enzymes (DUBs), which can serve to reverse the effects of ubiquitination (13, 14).

In recent years, we have examined inositol 1,4,5-trisphosphate (IP_3) receptor (IP_3R) processing by the UPP in intact cells (15). IP_3Rs are large (~260 kDa), ubiquitously expressed, ER membrane proteins that form tetrameric IP_3- and Ca^{2+}-regulated channels that govern Ca^{2+} release from the ER and are pivotal in mammalian cell signaling (16, 17). There are three IP_3R types (termed IP_3R1, IP_3R2, and IP_3R3) that form both homo- and heterotetramers and that have slightly different properties and markedly different tissue distributions. Remarkably, activation of certain cell-surface receptors that persistently elevate IP_3 concentration causes a decrease in

* This work was supported, in whole or in part, by National Institutes of Health Grants DK049194 (to R. J. H. W.) and GM67945 (to S. P. G.). This work was also supported by the American Heart Association (to D. A. S.).

[1] To whom correspondence should be addressed: Dept. of Pharmacology, SUNY Upstate Medical University, 750 E. Adams St., Syracuse, NY 13210. Tel.: 315-464-7956; Fax: 315-464-8014; E-mail: wojcikir@upstate.edu.

[2] The abbreviations used are: UPP, ubiquitin-proteasome pathway; ER, endoplasmic reticulum; DUB, deubiquitinating enzyme; IP_3, inositol 1,4,5-trisphosphate; IP_3R, IP_3 receptor; AQUA, absolute quantification; GnRH, gonadotropin-releasing hormone; Ub, ubiquitin.

cellular IP_3R levels (15). This process, termed "IP_3R down-regulation," is mediated by the UPP (18–22), occurs for all IP_3R types in a variety of cells and tissues (18, 20, 21), requires the proteins UBE2G2 (*Mus musculus* Ubc7) and p97 and the SPFH1/2 complex (23–25), and may serve to protect against the deleterious effects of prolonged Ca^{2+} release (15).

The value of examining ubiquitination in the context of intact cells, which contain a full complement of ubiquitinating enzymes and DUBs, rather than *in vitro* has been illustrated by some recent studies. For example, it was reported that *in vitro* ubiquitination of cyclin B_1 by the E3 anaphase-promoting complex and the E2 UbcH10 resulted in the formation of ubiquitin chains linked though Lys-48, Lys-63, and Lys-11 (9). However, utilization of UbcH10 plus UBE2S, which is the more physiological E2 module for the anaphase-promoting complex, *in vitro* and *in vivo* facilitated the specific catalysis of Lys-11-linked ubiquitin chains (11, 26, 27). Likewise, *in vitro* construction of ubiquitin chains using various E2-E3 pairs revealed the formation of non-degradable forked ubiquitin chains (28), whereas forked chains were no longer formed when the proteasomal subunit S5a was included (29). Finally, *in vitro*, epidermal growth factor receptors were modified by just monoubiquitin (30), whereas in intact cells, they were tagged with both monoubiquitin and Lys-63-linked ubiquitin chains (31). In each case, achieving more physiological conditions resulted in apparently more physiological results. IP_3Rs provide very appealing tools for studying the UPP under physiological conditions because endogenous receptors can be rapidly ubiquitinated through stimulation of endogenous signaling pathways in intact cells. Thus, we have employed a mass spectrometric technique called AQUA (for absolute quantification) (32, 33) and recently developed linkage-specific ubiquitin antibodies (34) to thoroughly assess the ubiquitination of IP_3R1–3 in several cell lines and have determined the roles of the attached ubiquitin chains in IP_3R degradation.

EXPERIMENTAL PROCEDURES

Materials—αT3-1 mouse pituitary cells, Rat1 fibroblasts, AR42J rat pancreatoma cells, and SHSY5Y human neuroblastoma cells were obtained and maintained as described previously (20, 22, 23). The antibodies used were as follows: affinity-purified rabbit polyclonal anti-IP_3R1, anti-IP_3R2, and anti-IP_3R3 (20); mouse monoclonal anti-IP_3R3 (TL3, BD Transduction Laboratories); anti-p97 (Research Diagnostics Inc.); anti-FLAG (clone M5, Sigma); anti-ubiquitin (clone FK2, BIOMOL); and humanized anti-Lys-48 and anti-Lys-63 linkage-specific antibodies (kindly provided by Genentech) (34). Gonadotropin-releasing hormone (GnRH), endothelin-1, cholecystokinin, carbachol, and *N*-ethylmaleimide were purchased from Sigma, and MG132 was purchased from BIOMOL. Reagents for immunoprecipitation, electrophoresis, and immunoblotting were obtained as described previously (22). The plasmids used encoded FLAG-UbWT (ubiquitin tagged at the N terminus with a FLAG epitope; a kind gift from I. Dikic) and FLAG-tagged ubiquitin mutants FLAG-UbK48R and FLAG-UbK63R, in which Lys residues were mutated to Arg residues by site-directed mutagenesis.

Immunoprecipitation for Mass Spectrometric Analysis—αT3-1, Rat1, AR42J, and SHSY5Y cells were grown to confluence in 15-cm diameter dishes, and 24 h prior to harvesting, Rat1 cells were cultured in serum-free medium. After stimulation, cells were harvested by the addition of ice-cold lysis buffer (3–6 ml/dish; 50 mM Tris, 150 mM NaCl, 1% Triton X-100, 1 mM EDTA, 0.2 mM phenylmethylsulfonyl fluoride, 10 μM pepstatin, and 0.2 μM soybean trypsin inhibitor, pH 8.0). Lysates were then incubated with 2.5 mM *N*-ethylmaleimide for 1 min to inhibit DUBs, quenched by the addition of 5 mM dithiothreitol, incubated at 4 °C for 30 min with occasional mixing, and cleared by centrifugation at 16,000 × *g* for 10 min at 4 °C. For immunoprecipitation, clarified lysate was incubated overnight at 4 °C with protein A-Sepharose CL-4B beads and rabbit polyclonal antibodies. Immune complexes were collected by centrifugation for 1–3 min at 3000 × *g*, washed three times with ice-cold lysis buffer, resuspended in gel loading buffer, incubated at 100 °C for 3 min, subjected to SDS-PAGE, and either Coomassie Blue-stained (rocked in 10% acetic acid, 40% ethanol, and 2.5 g/liter Coomassie Brilliant Blue R for 1 h) and destained (rinsed with 10% acetic acid and 40% ethanol for 30 min) or transferred to nitrocellulose and immunoblotted and analyzed as described previously (22).

Ubiquitin Site Identification and Ubiquitin AQUA Analysis—Regions corresponding to ubiquitinated IP_3Rs were excised from Coomassie Blue-stained gels and processed for mass spectral analysis as described previously (33). Trypsin digestion of ubiquitinated proteins generates peptides that have a covalently attached diglycine motif (resulting from digestion of ubiquitin between Arg-74 and Gly-75) at the modified lysine and a missed lysine cleavage at that lysine (32, 35). For IP_3R ubiquitination site identification, tandem mass spectra were searched using SeaQuest with a variable mass addition of 114.0429 Da in lysines to match the diglycine signature, and matches corresponding to IP_3R ubiquitination sites were validated based on the mass accuracy of the precursor ion and manual inspection of the tandem MS spectra. For AQUA analysis, the ion-extracted chromatogram was drawn with 10-ppm mass accuracy, and cell-derived ubiquitin peptides were quantified from the ratio of the area under the curve for these peptides *versus* that for ubiquitin-derived AQUA peptides (9, 32). Throughout AQUA analysis, conditions were optimized to avoid differences in reference peptide recovery as described (9, 32).

Immunoblotting and Immunoprecipitation using Anti-Lys-63 and Anti-Lys-48 Antibodies—Ubiquitin chains (purchased from BIOMOL) and cell lysates were mixed with gel loading buffer and incubated at 100 °C for 3 min prior to SDS-PAGE and immunoblotting. Antibody dilutions were adjusted to produce equal signals from the chain standards to allow for subsequent semiquantitative immunoblotting (~1:40, ~1:750, and ~1:750 for anti-Lys-48, anti-Lys-63, and anti-ubiquitin (FK2) antibodies, respectively). IP_3Rs immunopurified from stimulated αT3-1, AR42J, and Rat1 cells were incubated with gel loading buffer at 37 °C for 30 min prior to SDS-PAGE and immunoblotting.

For immunodepletion, IP_3R1 was immunopurified from stimulated αT3-1 cell lysates with anti-IP_3R1 antibody. IP_3R1 was eluted from anti-IP_3R1 antibody by incubation at 37 °C for 90 min in 1% Zwittergent plus the peptide (1 ng/μl) against which the antibody was raised (20) and 2 mM dithiothreitol, and the eluted IP_3R subunits were incubated overnight at 4 °C with anti-Lys-63 or anti-Lys-48 antibody plus 2 mg of protein A beads. After centrifugation, portions of the supernatants were incubated with gel loading buffer at 37 °C for 30 min and subjected to SDS-PAGE and immunoblotting.

Analysis of IP_3R Levels in Cell Lysates—αT3-1, Rat1, and AR42J cells were grown to confluence in BD Falcon 6-well dishes. After stimulation, cells were harvested in 200 μl of ice-cold lysis buffer, and cell lysates were mixed with gel loading buffer, boiled at 100 °C for 3 min, and subjected to SDS-PAGE and immunoblotting (22). IP_3R immunoreactivity was quantitated using a GeneGnome imager (Syngene).

Transfection of αT3-1 Cells by Electroporation—αT3-1 cells were transfected using the NEON transfection system (Invitrogen). Briefly, αT3-1 cells were trypsinized, washed with culture medium and then phosphate-buffered saline, and resuspended in Buffer R (Invitrogen) at 1.5×10^7 cells/ml. Cells were then mixed with cDNA (15 μg/1.5×10^6 cells), and 100-μl aliquots were electroporated (one pulse, 20 ms, 1.5 kV) and seeded into a well of a BD Falcon 12-well dish. 24 h later, cells were treated with 10 nM GnRH, and cell lysates were prepared and subjected to SDS-PAGE and immunoblotting.

RESULTS

All IP_3R Types Are Ubiquitinated in the Regulatory Domain—In our previous mass spectrometric analysis of IP_3R ubiquitination, we examined IP_3R1 isolated from GnRH-stimulated αT3-1 cells and found that at least 11 of the 167 lysines in IP_3R1 are ubiquitinated (33). The bulk of IP_3Rs reside in the cytosol and can be divided into three domains: the N-terminal ligand-binding domain, the central regulatory domain, and the C-terminal channel domain that contains six transmembrane helices and the channel pore (amino acids 1–576, 577–2276, and 2277–2749, respectively, for mouse IP_3R1) (16). All of the ubiquitination sites previously identified (33) are found in the regulatory domain and are near modulatory sites (*e.g.* for phosphorylation, ATP binding, etc.) or protease-sensitive sites, suggesting that they are all located in surface-exposed loops (36, 37).

To determine whether or not IP_3R2 and IP_3R3 are ubiquitinated similarly to IP_3R1, we examined IP_3R2 isolated from cholecystokinin-stimulated AR42J cells, which express 86% IP_3R2, 12% IP_3R1, and 2% IP_3R3 (20), and endothelin-1-stimulated Rat1 cells, which express ~50% IP_3R1 and ~50% IP_3R3 (23). Furthermore, to define whether IP_3R1 ubiquitination is context-dependent, we examined IP_3R1 isolated from SHSY5Y cells, which, like αT3-1 cells, contain >99% IP_3R1 (20).

In the absence of stimulus, little or no ubiquitin immunoreactivity was associated with IP_3Rs from αT3-1, Rat1, AR42J, and SHSY5Y cells (Fig. 1*A*, *lanes 1*, *3*, *5*, and *7*). However, upon treatment with the appropriate stimulus, IP_3Rs became ubiquitinated, as indicated by the presence of a smear of ubiquitin immunoreactivity beginning at ~270 kDa and extending upward (Fig. 1*A*, *lanes 2*, *4*, *6*, and *8*). To identify sites of ubiquitination and for AQUA analysis, regions corresponding to ubiquitinated IP_3Rs, excised from analogous Coomassie Blue-stained gels, were subjected to in-gel trypsin digestion and tandem MS (32).

Re-examination of ubiquitinated IP_3R1 from αT3-1 cells identified seven ubiquitination sites: Lys-916, Lys-1571, Lys-1771, Lys-1884, Lys-1899, Lys-1901, and Lys-1924 (Fig. 1*B*). Six of these were identified previously (33), whereas one, Lys-1899, is new. Six ubiquitination sites were identified in IP_3R2 from AR42J cells: Lys-909, Lys-1589, Lys-1722, Lys-1836, Lys-1864, and Lys-2071 (Fig. 1*B*). Only one IP_3R3 site, Lys-2100, was identified in Rat1 cells. As expected, ubiquitination sites for IP_3R1 were also identified in SHSY5Y cells (Lys-1847 and Lys-1870), Rat1 cells (Lys-916, Lys-962, and Lys-1771), and AR42J cells (Lys-916, Lys-1884, and Lys-1901) (Fig. 1*B*). Although ubiquitination sites were identified for IP_3R1 in all cell types, most were found in αT3-1 cells, most likely because IP_3R ubiquitination is particularly strong in αT3-1 cells (Fig. 1*A*), and this allowed for the identification of more ubiquitinated IP_3R1 peptides than in the other cell types. Indeed, it seems that the frequency of ubiquitination sites identified in IP_3R1, IP_3R2, and IP_3R3 in the different cell types reflects a combination of the relative abundance of each receptor type and the strength of stimulus-induced IP_3R ubiquitination (Fig. 1*A*).

Remarkably, every ubiquitination site identified, regardless of receptor type, is located within the IP_3R regulatory domain. More specifically, alignment suggests that, despite sequence differences between the receptor types, ubiquitination sites appear to be clustered in the vicinity of putative surface-exposed loops, *i.e.* near regulatory or protease-sensitive sites (Fig. 1*C*). For example, Lys-909 of IP_3R2 from AR42J cells aligns near Lys-916 of IP_3R1 from αT3-1, AR42J, and Rat1 cells, and these lysines are located near a protease cleavage site (Arg-922 in IP_3R1 and between Ser-916 and Ser-934 in IP_3R3) (37, 38) and near PKA phosphorylation sites (Ser-916 and Ser-934 in IP_3R3 and Ser-937 in IP_3R2) (38, 39) (Fig. 1*C*). Likewise, Lys-1771 of IP_3R1 from αT3-1 and Rat1 cells aligns with Lys-1722 of IP_3R2 from AR42J cells and is found in a glycine-rich region that, in IP_3R1, contains an ATP-binding site (positions 1773–1775) and is thought to form a flexible connector between the cytosolic and membrane portions of IP_3Rs (16). Finally, a cluster of ubiquitination sites is found close to the first transmembrane domain (Fig. 1*C*): Lys-1884, Lys-1899, Lys-1901, and Lys-1924 of IP_3R1 and Lys-1836 and Lys-1864 of IP_3R2 flank an IP_3R1 caspase-3 cleavage site (Asp-1891), an IP_3R3 PKA phosphorylation site (Ser-1834), and an IP_3R1 protease cleavage site (Arg-1931) (37). The one ubiquitination site identified in IP_3R3, Lys-2100, is also located in this region.

In summary, all ubiquitination sites identified localize to probable surface-exposed loops in the IP_3R regulatory domain, and for at least IP_3R1, selection of sites seems to be context-independent because homologous aligning lysines were frequently selected in different cell types (*e.g.* Lys-1847 in SHSY5Y cells and Lys-1901 in αT3-1 cells). Similarly, com-

A

Cell Type	αT3-1		Rat1		AR42J		SHSY5Y	
$IP_3R1:2:3$ content	99:0:1		50:0:50		12:86:2		99:1:0	
IP antibody	IP_3R1		IP_3R1+3		IP_3R1+2		IP_3R1	
Stimulus	-	+	-	+	-	+	-	+
Lane	1	2	3	4	5	6	7	8

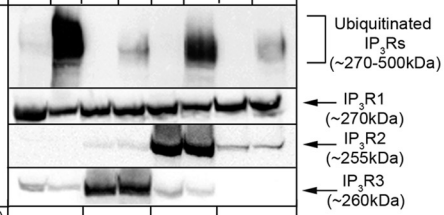

Total Ubiquitin (fmol) with stimulus		3684.5	1109.8	3809.5	810.8
Unmodified Ubiquitin (% of total)		68.2	71.0	70.2	71.3
Modified Ubiquitin (% of total)		31.8	29.0	29.8	28.7
Specific linkages (% of total)	K48	9.8	3.5	4.1	6.3
	K63	17.8	23.0	21.1	18.9
	other linkages	4.0	2.5	4.5	3.5

B

Cell Type (Species)	IP_3R Type	Amino Acid Number	Peptide Sequence
αT3-1 (Mm)	R1	K916	K.GEENK^GSNVMR.S
	R1	K1571	K.SHNIVQK^TALNWR.L
	R1	K1771	R.ESTSFGNGPLSPGGPSK^PGGGGGGPGSSSTSR.G
	R1	K1884	K.ATVTVNTSDLGNK^K.K
	R1	K1899, K1901	K.K^AK^EPTTQITEEVR.D
	R1	K1901	K.AK^EPTTQITEEVR.D
	R1	K1924	R.K^AFTTFR.R
SHSY5Y (Hs)	R1	K1847	K.AK^EPTTQITEEVR.D
	R1	K1870	R.K^AFTTFR.R
Rat1 (Rn)	R1	K916	K.GEENK^GSNVMR.S
	R1	K962	K.QAEPEK^EDIMVMDTK.L
	R1	K1771	R.ESLTSFGNGPLSPGGPSK^PGGGGGGPGSGSTSR.G
AR42J (Rn)	R1	K916	K.GEENK^GSNVMR.S
	R1	K1884	K.ATVTVNTSDLGNK^K.K
	R1	K1901	K.AK^EPTTQITEEVR.D
	R2	K909	R.LSK^FQDGSNNVMR.T
	R2	K1589	R.FK^EALGGPAWDYR.N
	R2	K1722	K.GDHSVGVNGPLSGAYAK^TAQGGGFTGQDADK.T
	R2	K1836	K.K^REEDSDLMALGPR.M
	R2	K1864	K.EGMK^GQLTEASSATAK.A
	R2	K2071	R.PK^ELVDMK.N
Rat1 (Rn)	R3	K2100	K.QLSQMLK^SSAPAQEEEEDPLAYYENHYSQIEIVR.Q

C

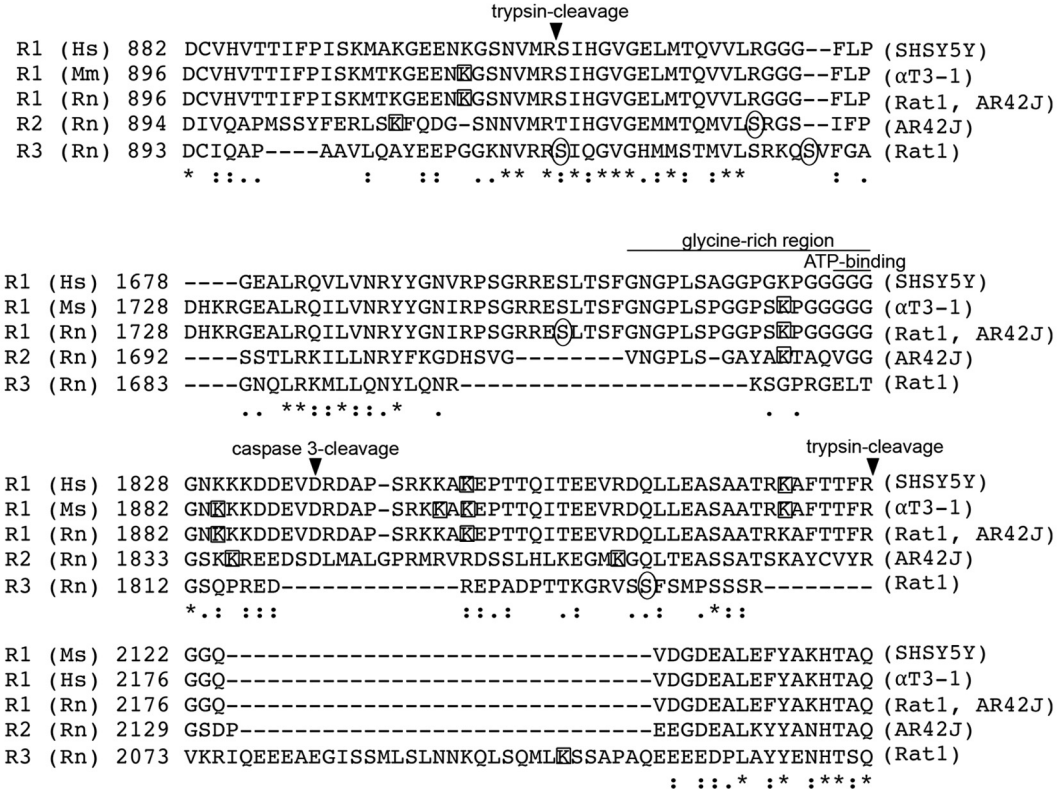

FIGURE 1. **Identification of IP_3R ubiquitination sites by mass spectrometry.** *A*, αT3-1 cells (*lanes 1* and *2*) were incubated without or with 100 nM GnRH for 7 min; Rat1 cells (*lanes 3* and *4*) were incubated without or with 10 nM endothelin-1 for 10 min; AR42J cells (*lanes 5* and *6*) were incubated without or with 200 nM cholecystokinin for 20 min; and SHSY5Y cells (*lanes 7* and *8*) were incubated without or with 1 mM carbachol for 20 min. Cell lysates were prepared, and IP_3Rs were immunopurified (*IP*) with the antibodies indicated. Samples were electrophoresed by 5% SDS-PAGE and either Coomassie Blue-stained (not shown) or transferred to nitrocellulose and probed with anti-IP_3R1, anti-IP_3R2, anti-IP_3R3 (TL3), and anti-ubiquitin (FK2) antibodies. The *bracket* locates ubiquitinated IP_3Rs, and *arrows* indicate IP_3R1, IP_3R2, and IP_3R3. Numerical mass spectrometric data are presented as percent of total ubiquitin. *B*, listed are the ubiquitination sites identified from αT3-1, Rat1, AR42J, and SHSY5Y cells together with the peptides that contain the modified lysines. The *periods* indicate trypsin cleavage sites, and the *carets* indicate ubiquitination sites. *C*, multiple sequence alignments for human, mouse, and rat IP_3R1 and rat IP_3R2 and IP_3R3 were performed by ClustalW. Selected portions are shown with ubiquitination sites *boxed*. Known sites of PKA phosphorylation for IP_3R1, IP_3R2, and IP_3R3 are *circled*. Trypsin and caspase-3 cleavage sites are indicated by *arrowheads*, and a glycine-rich region and an IP_3R1 ATP-binding site are also shown. *Asterisks* indicate completely conserved residues; *colons* indicate highly conserved residues; and *periods* indicate moderately conserved residues. *Hs*, *Homo sapiens*; *Mm*, *Mus musculus*; *Rn*, *Rattus norvegicus*.

paring IP_3R1 and IP_3R2, lysines selected for ubiquitination were frequently aligned, despite sequence variation around these lysines.

IP_3Rs from All Cell Types Are Tagged with the Same Ubiquitin Conjugates but in Different Proportions—AQUA analysis of ubiquitinated IP_3Rs immunopurified from stimulated

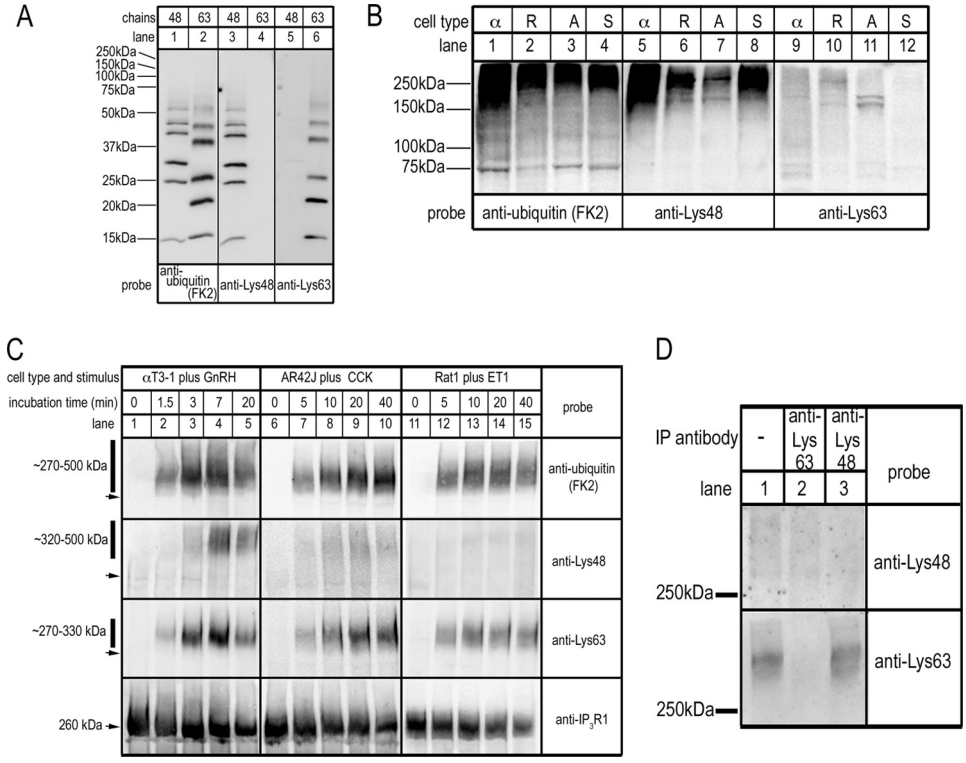

FIGURE 2. **IP_3Rs are tagged with homogeneous Lys-48- and Lys-63-linked ubiquitin chains.** Lys-48- or Lys-63-linked ubiquitin chains two to seven residues in length (250 ng) (*A*) or lysates from αT3-1 (α), Rat1 (*R*), AR42J (*A*), or SHSY5Y (*S*) cells (*B*) were subjected to 12% SDS-PAGE and probed with anti-ubiquitin (FK2), anti-Lys-48, or anti-Lys-63 antibody. Antibody dilutions were adjusted to produce equal signals from standard amounts of Lys-48- and Lys-63-linked chains. *C*, αT3-1, Rat1, and AR42J cells were treated with 100 nM GnRH, 10 nM endothelin-1 (*ET1*), or 200 nM cholecystokinin (*CCK*) for the times indicated, and IP_3Rs were immunopurified as described in the legend for Fig. 1*A*, separated by 5% SDS-PAGE, and probed as described for *A*. *D*, αT3-1 cells were treated with 100 nM GnRH for 7 min, and cell lysates were incubated with anti-IP_3R1 antibody to isolate IP_3R1. Immunoprecipitated (*IP*) IP_3R1 was eluted from beads and incubated without antibody (*lane 1*) or with anti-Lys-63 (*lane 2*) or anti-Lys-48 (*lane 3*) antibody, and immunodepleted supernatants were subjected to SDS-PAGE, transferred to nitrocellulose, and probed for Lys-48 and Lys-63 linkage immunoreactivity.

αT3-1, Rat1, AR42J, and SHSY5Y cells revealed that, in all cell types, the bulk of ubiquitin associated with IP_3Rs (~70% of total ubiquitin) was unmodified, *i.e.* either monoubiquitin or end cap ubiquitin (the last ubiquitin in a chain), and that the remaining ~30% was modified, *i.e.* ubiquitin that forms chain linkages (Fig. 1*A*). This indicates that, at a minimum, ~40% of IP_3R-conjugated ubiquitin is monoubiquitin because if chains are assumed to consist of just two ubiquitin moieties, then 60% of total ubiquitin would be involved in chains. If, as is probable, chains are longer than two ubiquitin moieties, then >40% will be monoubiquitin (33). Consistent with our previous work (33), the vast majority of the chain linkages were via Lys-48 and Lys- 63, and only minimal amounts of the other linkages were found (Fig. 1*A*). Although the ratio of unmodified to modified ubiquitin attached to IP_3Rs was approximately constant in each cell type, the ratio of Lys-63 to Lys-48 linkages varied considerably: 6.6:1, 5.1:1, 3.0:1, and 1.8:1 in Rat1, AR42J, SHSY5Y, and αT3-1 cells, respectively (Fig. 1*A*). Notably, the total femtomoles of ubiquitin that accumulated on IP_3Rs correlated with the intensity of the ubiquitin immunoreactivity observed by immunoblotting (Fig. 1*A*).

We next sought to determine the kinetics of ubiquitin chain formation using recently described linkage-specific antibodies (34). As indicated in Fig. 2*A*, these antibodies showed the appropriate specificity toward Lys-48- and Lys-63-linked chains (*lanes 3–6*), whereas anti-ubiquitin antibody (FK2) recognized both chain types (*lanes 1* and *2*). It was also immediately apparent in all cell types examined that Lys-48 linkages were much more abundant than Lys-63 linkages (Fig. 2*B*, compare *lanes 5–8* with *lanes 9–12*).

Fig. 2*C* shows time courses of IP_3R ubiquitination in αT3-1, Rat1, and AR42J cells measured with FK2 and anti-Lys-48 and anti-Lys-63 antibodies. Importantly, for αT3-1 cells, the changes in Lys-48 and Lys-63 linkage immunoreactivity (Fig. 2*C*, *lanes 1–5*) paralleled the changes in Lys-48 and Lys-63 linkage abundance measured by mass spectrometry (33), most notably with Lys-63 linkage immunoreactivity increasing more rapidly than Lys-48 linkage immunoreactivity. Clearly then, these antibodies provide an effective way to assess Lys-48 and Lys-63 linkage addition to IP_3Rs and have an advantage over mass spectrometry in that they allow for the ubiquitination status of a large number of samples to be rapidly assessed by immunoblotting. Application of these antibodies to IP_3Rs immunoprecipitated from Rat1 and AR42J cells (Fig. 2*C*, *lanes 6–15*) showed that Lys-63 linkages accumulated rapidly and, consistent with mass spectrometry, were much more abundant than Lys-48 linkages. Overall, these data show that, in all cell types examined, activated IP_3Rs are modified with both Lys-48- and Lys-63-linked ubiquitin chains and that, at least in αT3-1 cells, Lys-63 linkages accumulate most rapidly and that, in AR42J and Rat1 cells, the

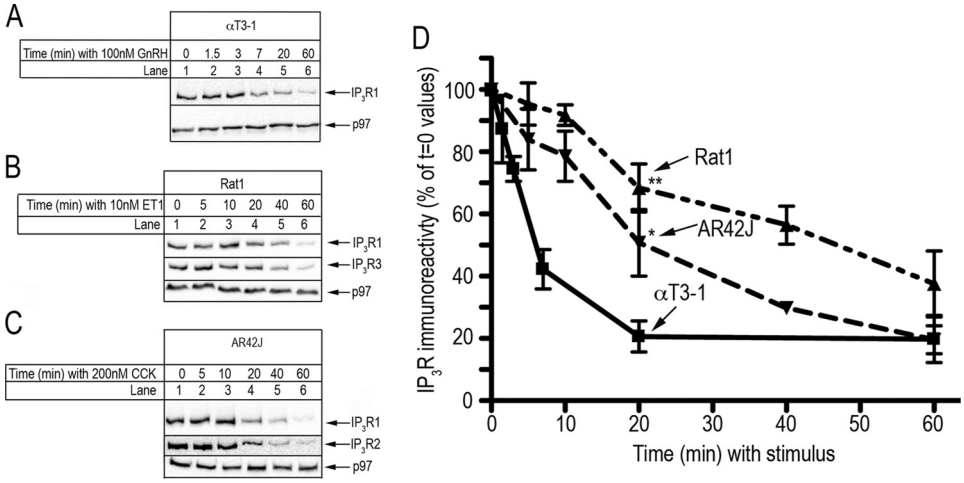

FIGURE 3. **IP_3Rs are degraded at different rates in different cell types.** *A–C*, αT3-1, Rat1, and AR42J cells were stimulated as indicated, and cell lysates were subjected to 7% SDS-PAGE, transferred to nitrocellulose, and probed for IP_3Rs. Lysates were also probed for p97 as a loading control. *ET1*, endothelin-1; *CCK*, cholecystokinin. *D*, graph of IP_3R levels in αT3-1, Rat1, and AR42J cells. Immunoreactivity of the bands corresponding to unmodified IP_3R1, IP_3R2, and IP_3R3 (at 270, 255, and 260 kDa, respectively) was quantified and normalized to $t = 0$ values. For Rat1 and AR42J cells, values for both IP_3R types were averaged. Data presented are the mean ± S.E. ($n > 3$). *, $p < 0.05$; **, $p < 0.01$ (comparing AR42J cell and Rat1 cell immunoreactivity with αT3-1 cell immunoreactivity at 20 min).

vast majority of ubiquitin chains are coupled by Lys-63 linkages.

IP_3Rs Are Tagged with Homogeneous Lys-48- and Lys-63-linked Ubiquitin Chains—Remarkably, it was consistently the case that for immunopurified ubiquitinated IP_3Rs, anti-Lys-48 immunoreactivity (~320–500 kDa) migrated at a higher molecular mass than anti-Lys-63 immunoreactivity (~270–330 kDa) (Fig. 2*C*). This observation was most readily detected in αT3-1 cells, where Lys-48 linkages are most abundant, and is highly significant, as it indicates (i) that Lys-48 and Lys-63 linkages are segregated into different chains and (ii) that Lys-48 and Lys-63 linkages are not on the same IP_3R subunits (if the converse of either of these points was true, then Lys-48 and Lys-63 immunoreactivity would co-migrate). To directly address these assertions, we used anti-Lys-63 and anti-Lys-48 antibodies to immunodeplete purified ubiquitinated IP_3R1 subunits (Fig. 2*D*). In the absence of immunodepleting antibody, Lys-48 and Lys-63 immunoreactivity associated with purified IP_3R1 remained in solution (*lane 1*), whereas inclusion of either anti-Lys-63 or anti-Lys-48 antibody effectively removed all the Lys-63 and Lys-48 linkage immunoreactivity, respectively (*lanes 2* and *3*). However, anti-Lys-63 antibody did not deplete Lys-48 linkage immunoreactivity, nor did anti-Lys-48 antibody deplete Lys-63 linkage immunoreactivity (*lanes 2* and *3*), confirming that homogeneous Lys-48- and Lys-63-linked chains are segregated onto separate IP_3R subunits.

IP_3R Degradation Occurs More Rapidly in αT3-1 Cells than in Rat1 and AR42J Cells—In view of the differences in the Lys-63/Lys-48 linkage ratio between αT3-1, AR42J, and Rat1 cells and the canonical role of Lys-48-linked chains in triggering proteasomal degradation, we wondered whether the rate of IP_3R degradation varied between the different cell types. To test this, αT3-1, Rat1, and AR42J cells were stimulated, and cell lysates were assessed for IP_3R content (Fig. 3, *A--C*); the immunoreactivity of bands corresponding to unmodified IP_3Rs was used to quantitate IP_3R levels because only a small proportion of receptors (<10%) are ubiquitinated at any one time in maximally stimulated cells (22), and this small proportion is not readily detectable in immunoblots of cell lysates. IP_3R degradation occurred most rapidly in αT3-1 cells, with IP_3R1 levels being maximally depleted to 21 ± 5% of basal levels after 20 min (Fig. 3*D*). In contrast, IP_3R depletion in AR42J and Rat1 cells was less rapid, and after 20 min, IP_3R levels were 51 ± 11 and 68 ± 8% of basal levels, respectively (Fig. 3*D*). Thus, the IP_3R1 degradation rate does correlate with the abundance of Lys-48-linked chains attached to IP_3Rs, and the lower the Lys-63/Lys-48 linkage ratio (Figs. 1*A* and 2*C*), the faster the degradation rate.

Proteasomal Inhibition Causes More Lys-48-linked Ubiquitin than Lys-63-linked Ubiquitin to Accumulate on IP_3R1—We also wondered whether proteasomal inhibition might provide insight into the relative importance of Lys-48- and Lys-63-linked chains in triggering IP_3R degradation. In αT3-1 cells, IP_3Rs were degraded very rapidly, with levels depleted to 42 ± 6% of basal levels after 7 min (Fig. 3, *A* and *D*); correspondingly, ubiquitination was maximal at 7 min (Fig. 2*C*). We have shown previously that the proteasomal inhibitor MG132 acts very rapidly to inhibit the proteasome and to block IP_3R1 degradation in αT3-1 cells (22). Thus, αT3-1 cells were exposed to GnRH for 7 min either without or with MG132, and Lys-48 and Lys-63 linkage levels were assessed (Fig. 4*A*). Remarkably, proteasomal inhibition caused a greater increase in accumulation of Lys-48-linked ubiquitin on IP_3Rs than Lys-63-linked ubiquitin (80 *versus* 8%, respectively) (Fig. 4*B*), suggesting that Lys-48-conjugated IP_3Rs are degraded by the proteasome but that Lys-63-conjugated IP_3Rs are not.

Lys-48- but Not Lys-63-linked Ubiquitin Chains Are Required for IP_3R1 Degradation—To directly assess the role of Lys-48- and Lys-63-linked ubiquitin in IP_3R degradation, we generated FLAG-tagged ubiquitin mutants containing lysine-to-arginine mutations to prevent the formation of either Lys-48- or Lys-63-linked ubiquitin chains (FLAG-UbK48R or

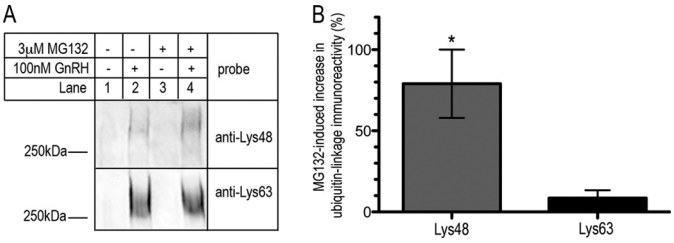

FIGURE 4. **Effects of MG132 on ubiquitin chain accumulation on IP_3Rs.** *A*, αT3-1 cells were treated without or with GnRH and MG132 for 7 min as indicated, and IP_3R1 was immunoprecipitated and probed as described in the legend for Fig. 2*C*. *B*, graph of the MG132-induced increase in Lys-48 and Lys-63 immunoreactivity obtained from quantitation of *lanes 2* and *4* in *A*. Data presented are the mean ± S.E. ($n = 3$). *, $p < 0.05$.

FLAG-UbK63R, respectively) and overexpressed these or wild-type FLAG-tagged ubiquitin (FLAG-UbWT) in αT3-1 cells (Fig. 5). Using standard lipid-based or Ca^{2+} phosphate transfection methods, it has been impossible to obtain high transfection efficiency in αT3-1 cells (22), but using electroporation, significant overexpression was achieved, as indicated by the appearance of FLAG immunoreactivity (Fig. 5*A*, *lanes 2–4*) and an ~2.4-fold increase in total ubiquitin immunoreactivity when FLAG-UbWT, FLAG-UbK48R, and FLAG-UbK63R were expressed (*lanes 5–8*). In FLAG-UbWT- and FLAG-UbK63R-transfected cells, IP_3R1 degradation proceeded with similar kinetics, and levels declined to 48 ± 7 and 40 ± 10% of basal levels, respectively, after 1 h (Fig. 5, *B* and *C*). In contrast, IP_3R1 degradation was completely inhibited when FLAG-UbK48R was overexpressed (Fig. 5, *B* and *C*). Thus, only Lys-48-linked ubiquitin chains, but not Lys-63-linked ubiquitin chains, can trigger the degradation of IP_3Rs. Furthermore, these data rule out a role for the monoubiquitin attached to IP_3Rs in IP_3R degradation because both of the ubiquitin mutants allowed for monoubiquitination.

DISCUSSION

Using mass spectrometry and linkage-specific antibodies to characterize IP_3R ubiquitination, we have found (i) that all IP_3R types are subject to ubiquitination at approximately the same locations independent of cellular context; (ii) that independent of cell type, IP_3Rs are modified mainly by monoubiquitin, with the remainder attached as Lys-48- and Lys-63-linked ubiquitin chains; (iii) that the attached ubiquitin chains are homogeneous; and (iv) that the Lys-48-linked ubiquitin chains, but not the Lys-63-linked chains, are required for IP_3R degradation. For all IP_3R types, ubiquitination appears to be confined to the regulatory domain (amino acids 577–2276 for mouse IP_3R1). The regulatory domain is the large central region of IP_3Rs that contains myriad binding sites for modifiers, including a Ca^{2+}-binding site that is critical for IP_3R activity, and sites of phosphorylation (16, 40). IP_3R structure solved to 30 Å by cryo-electron microscopy and single particle analysis predicts that this domain forms the outer surface of the IP_3R tetramer (41, 42). This (and the close proximity of ubiquitinated lysines to sites of modification or protease cleavage sites) suggests that surface-exposed lysines are predominately selected for ubiquitination. Given that ubiquitinated lysines were often in close proximity when IP_3R sequences were aligned but that there was considerable sequence variance

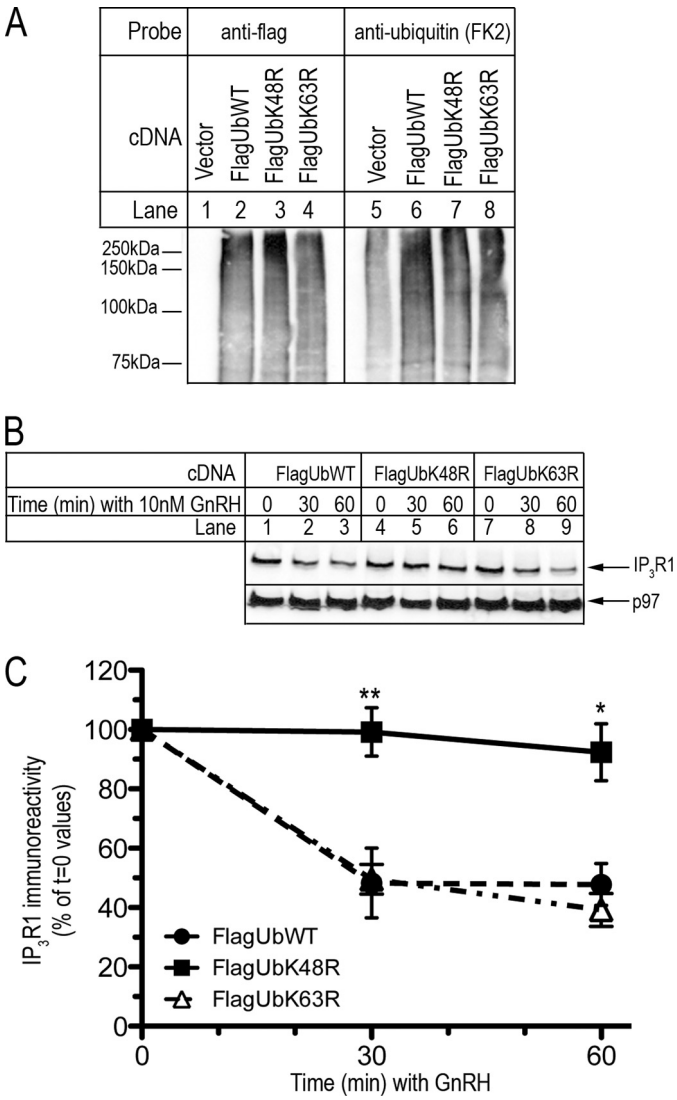

FIGURE 5. **Lys-48-linked ubiquitin chains, but not Lys-63-linked ubiquitin chains, are required for the degradation of endogenous IP_3R1.** *A*, αT3-1 cells were transfected with vector (pcDNA3) or the constructs indicated, and 24 h later, cell lysates were prepared, subjected to 7% SDS-PAGE, transferred to nitrocellulose, and probed with anti-FLAG or anti-ubiquitin (FK2) antibody. *B*, αT3-1 cells were transfected as described for *A* and then treated with 10 nM GnRH for 0, 30, or 60 min. Cell lysates were prepared, subjected to 7% SDS-PAGE, transferred to nitrocellulose, and probed with anti-IP_3R1 or anti-p97 antibody (as a loading control). *C*, graphed values of quantified IP_3R1 immunoreactivity. In each independent experiment, immunoreactivity was normalized to $t = 0$ values, and then normalized values were averaged. Data are presented as the mean ± S.E. ($n \geq 3$). *, $p < 0.01$; **, $p < 0.001$ (comparing mutant ubiquitin-expressing cells with FLAG-UbWT-expressing cells).

between IP_3Rs in the vicinity of targeted lysines, it seems that selection is based primarily on structural parameters, chiefly surface accessibility, rather than sequence.

Although we identified ubiquitination sites only in the regulatory domain, this does not exclude the possibility that lysines outside this domain may become ubiquitinated because inefficient ubiquitination or technical reasons could force signals from outside the regulatory domain to below the limits of detection. Likewise, whereas it is possible that Lys-2100 is the only site of ubiquitination in IP_3R3, it is more likely that the low abundance of ubiquitinated IP_3R3 precluded the identification of additional ubiquitinated lysines.

Irrespective of cultured cell type (and rat brain and pancreas tissues (data not shown)), IP_3Rs were modified by a mixture of monoubiquitin and ubiquitin chains, linked predominately through Lys-48 and Lys-63. Remarkably, using linkage-specific antibodies, we found that the vast majority and perhaps all ubiquitin chains are homogeneous, *i.e.* individual chains are composed entirely of either Lys-48 linkages or Lys-63 linkages, and that these homogeneous chains are segregated to distinct IP_3R subunits.

For proteins, such as IP_3Rs, that are tagged with multiple ubiquitin chain linkages, defining chain topology has proven to be very challenging (6), and for this reason, it has been generally assumed that the different linkages are segregated into homogeneous chains (5). Heterogeneous chains can certainly be formed *in vitro*, but as already explained in the Introduction, such conjugates may not be physiological. To the best of our knowledge, MHC class I is the only protein in addition to IP_3Rs to have its ubiquitin chain topology mapped *in vivo* (43, 44). Interestingly, MHC class I appears to be tagged with heterogeneous ubiquitin chains built with Lys-11 and Lys-63 linkages, both of which are required for the effective internalization and degradation of MHC class I (43, 44). This contrasts markedly with the situation for IP_3Rs and demonstrates that, in intact cells, ubiquitination is very complex, and it is unlikely that generalized "rules" regarding the formation of ubiquitin chains will emerge but rather that the topology of chains will have to be assessed for individual substrates.

The tagging of IP_3Rs with homogeneous chains raises several interesting points. First, as it is improbable that one E2/E3 pair could catalyze the formation of both homogeneous Lys-48- and Lys-63-linked chains, it is likely that more than one E2 and/or E3 is responsible for IP_3R ubiquitination. In this regard, there is mounting evidence and growing acceptance that E2 proteins determine linkage specificity in chain formation (reviewed in Ref. 45). Indeed, the E2 proteins UBE2S and UBE2G2 (Ubc7) and the UBE2N-UBE2V1 complex have been shown to catalyze Lys-11-, Lys-48-, and Lys-63-linked chains, respectively (27, 45–48). In our previous work, we found that overexpressing dominant-negative UBE2G2 partially blocked IP_3R ubiquitination and completely inhibited IP_3R degradation (25). Together, these data raise the possibility that UBE2G2 may be catalyzing the formation of Lys-48-linked chains on IP_3Rs and that an as yet unidentified E2 catalyzes the formation of Lys-63-linked chains. Furthermore, it is remarkable that Lys-48- and Lys-63-linked chains are segregated to separate IP_3R subunits. This segregation suggests a high degree of coordination between the enzymes catalyzing ubiquitination, and clearly, to move forward, it will be necessary to identify and characterize all of the relevant enzymes involved in IP_3R ubiquitination.

Second, the presence of homogeneous Lys-48- and Lys-63-linked ubiquitin chains suggests that each chain type may signal for a distinct function. Our data obtained using ubiquitin mutants show that Lys-48-linked chains, but not Lys-63-linked chains, are required for IP_3R degradation. Consistent with this point, we also found that proteasomal inhibition causes a significant increase in Lys-48-conjugated IP_3Rs (suggesting that Lys-48-conjugated IP_3Rs are normally degraded by the proteasome) and that IP_3Rs are degraded most rapidly in cells in which IP_3Rs are heavily modified with Lys-48-linked chains. Thus, Lys-48-linked chains are necessary and sufficient to trigger IP_3R degradation, whereas Lys-63-linked chains appear not to be involved in this process. What then might be the role of Lys-63-linked chains? In general, it appears that the information encoded by the various types of ubiquitin conjugates is transmitted by proteins containing specialized ubiquitin-binding domains (reviewed in Ref. 49). Although there are >20 families of proteins that contain ubiquitin-binding domains with affinities for various conjugates, several are known to interact with just Lys-63-linked chains. For example, RAP80 specifically binds Lys-63-linked chains and recruits BRCA1 to sites of DNA damage to facilitate activation of DNA damage repair pathways (50, 51). Thus, the Lys-63-linked chains attached to IP_3Rs could recruit additional regulatory proteins to IP_3Rs or, more globally, to the ER membrane. Likewise, the monoubiquitin conjugated to IP_3Rs does not directly mediate IP_3R degradation and could also play a recruiting role. It is also significant to note that, although Lys-11 linkages have recently been shown to mediate the proteasomal degradation of certain substrates (11, 12), we found only minimal amounts of Lys-11 linkages on activated IP_3Rs (Fig. 1*A*) (33), and they do not appear to play a role in IP_3R processing.

It is interesting to note that, although Lys-63-linked chains do not mediate IP_3R degradation, Lys-63 linkage levels peak and decline similarly to Lys-48 linkage levels (Fig. 2*C*). The decline in Lys-48 linkage levels can be readily attributed to proteasomal degradation of Lys-48-conjugated IP_3Rs, but the reason for the decline in Lys-63 linkage levels is less obvious. Most likely, this decline is mediated by DUBs because this is the only known method for removing ubiquitin from proteins (13, 14). Deubiquitination "rescues" proteins from the physiological consequence of ubiquitination, be it degradation or involvement in other cellular processes (14). Thus, Lys-63 linkage disassembly could simply serve to "shut off" signaling through Lys-63 linkages on IP_3Rs or, alternatively or in addition, Lys-63-linked chain removal could precede and allow for the reubiquitination of IP_3Rs with Lys-48-linked chains for the purpose of degradation. Significantly, there are already several known instances of this type of opposing deubiquitination-ubiquitination activity (34, 52–55). For example, using mass spectrometry and linkage-specific antibodies, it was shown recently that ErbB2 is tagged with Lys-48- and Lys-63-linked ubiquitin chains and that Lys-63-linked ubiquitin chains are edited by the DUB Usp9x (55). Remarkably, Lys-48-linked chains signal for the rapid degradation of ErbB2 by the proteasome, whereas Lys-63-linked chains signal for trafficking of ErbB2 to the lysosome (55). This reveals a highly complex, tightly controlled ubiquitin-dependent mechanism for the regulation of ErbB2 and seems similar to the situation we have described for IP_3Rs.

In light of our data and in line with current opinions in the ubiquitin field, we propose a model that explains the complexities of IP_3R ubiquitination in intact cells. First, activated IP_3Rs are tagged either with homogeneous Lys-48- or Lys-63-linked ubiquitin chains through the action of, at minimum,

two E2 proteins and perhaps multiple E3 proteins. Lys-48-conjugated IP_3Rs are then rapidly degraded by the proteasome, whereas Lys-63-conjugated IP_3Rs are not, and perhaps act to recruit proteins to IP_3Rs or the ER. Simultaneously, DUBs disassemble Lys-63-linked ubiquitin chains, and the rescued IP_3Rs are either retagged with Lys-63-linked chains or tagged with Lys-48-linked chains to trigger degradation.

Acknowledgments—We thank Justine Lu and Yuan Wang for many helpful discussions and Donald Kirkpatrick and Kazuishi Kubota for advice and efforts early in this project.

REFERENCES

1. Jung, T., Catalgol, B., and Grune, T. (2009) *Mol. Aspects Med.* **30,** 191–296
2. Vembar, S. S., and Brodsky, J. L. (2008) *Nat. Rev. Mol. Cell Biol.* **9,** 944–957
3. Finley, D. (2009) *Annu. Rev. Biochem.* **78,** 477–513
4. Weissman, A. M. (2001) *Nat. Rev. Mol. Cell Biol.* **2,** 169–178
5. Komander, D. (2009) *Biochem. Soc. Trans.* **37,** 937–953
6. Ikeda, F., and Dikic, I. (2008) *EMBO Rep.* **9,** 536–542
7. Pickart, C. M., and Fushman, D. (2004) *Curr. Opin. Chem. Biol.* **8,** 610–616
8. Thrower, J. S., Hoffman, L., Rechsteiner, M., and Pickart, C. M. (2000) *EMBO J.* **19,** 94–102
9. Kirkpatrick, D. S., Hathaway, N. A., Hanna, J., Elsasser, S., Rush, J., Finley, D., King, R. W., and Gygi, S. P. (2006) *Nat. Cell Biol.* **8,** 700–710
10. Saeki, Y., Kudo, T., Sone, T., Kikuchi, Y., Yokosawa, H., Toh-e, A., and Tanaka, K. (2009) *EMBO J.* **28,** 359–371
11. Williamson, A., Wickliffe, K. E., Mellone, B. G., Song, L., Karpen, G. H., and Rape, M. (2009) *Proc. Natl. Acad. Sci. U.S.A.* **106,** 18213–18218
12. Xu, P., Duong, D. M., Seyfried, N. T., Cheng, D., Xie, Y., Robert, J., Rush, J., Hochstrasser, M., Finley, D., and Peng, J. (2009) *Cell* **137,** 133–145
13. Love, K. R., Catic, A., Schlieker, C., and Ploegh, H. L. (2007) *Nat. Chem. Biol.* **3,** 697–705
14. Ventii, K. H., and Wilkinson, K. D. (2008) *Biochem. J.* **414,** 161–175
15. Wojcikiewicz, R. J., Pearce, M. M., Sliter, D. A., and Wang, Y. (2009) *Cell Calcium* **46,** 147–153
16. Foskett, J. K., White, C., Cheung, K. H., and Mak, D. O. D. (2007) *Physiol. Rev.* **87,** 593–658
17. Mikoshiba, K. (2007) *J. Neurochem.* **102,** 1426–1446
18. Bokkala, S., and Joseph, S. K. (1997) *J. Biol. Chem.* **272,** 12454–12461
19. Oberdorf, J., Webster, J. M., Zhu, C. C., Luo, S. G., and Wojcikiewicz, R. J. H. (1999) *Biochem. J.* **339,** 453–461
20. Wojcikiewicz, R. J. H. (1995) *J. Biol. Chem.* **270,** 11678–11683
21. Wojcikiewicz, R. J., Ernst, S. A., and Yule, D. I. (1999) *Gastroenterology* **116,** 1194–1201
22. Wojcikiewicz, R. J., Xu, Q., Webster, J. M., Alzayady, K., and Gao, C. (2003) *J. Biol. Chem.* **278,** 940–947
23. Alzayady, K. J., Panning, M. M., Kelley, G. G., and Wojcikiewicz, R. J. H. (2005) *J. Biol. Chem.* **280,** 34530–34537
24. Pearce, M. M., Wormer, D. B., Wilkens, S., and Wojcikiewicz, R. J. H. (2009) *J. Biol. Chem.* **284,** 10433–10445
25. Webster, J. M., Tiwari, S., Weissman, A. M., and Wojcikiewicz, R. J. H. (2003) *J. Biol. Chem.* **278,** 38238–38246
26. Jin, L., Williamson, A., Banerjee, S., Philipp, I., and Rape, M. (2008) *Cell* **133,** 653–665
27. Matsumoto, M. L., Wickliffe, K. E., Dong, K. C., Yu, C., Bosanac, I., Bustos, D., Phu, L., Kirkpatrick, D. S., Hymowitz, S. G., Rape, M., Kelley, R. F., and Dixit, V. M. (2010) *Mol. Cell* **39,** 477–484
28. Kim, H. T., Kim, K. P., Lledias, F., Kisselev, A. F., Scaglione, K. M., Skowyra, D., Gygi, S. P., and Goldberg, A. L. (2007) *J. Biol. Chem.* **282,** 17375–17386
29. Kim, H. T., Kim, K. P., Uchiki, T., Gygi, S. P., and Goldberg, A. L. (2009) *EMBO J.* **28,** 1867–1877
30. Mosesson, Y., Shtiegman, K., Katz, M., Zwang, Y., Vereb, G., Szollosi, J., and Yarden, Y. (2003) *J. Biol. Chem.* **278,** 21323–21326
31. Huang, F., Kirkpatrick, D., Jiang, X., Gygi, S., and Sorkin, A. (2006) *Mol. Cell* **21,** 737–748
32. Kirkpatrick, D. S., Gerber, S. A., and Gygi, S. P. (2005) *Methods* **35,** 265–273
33. Sliter, D. A., Kubota, K., Kirkpatrick, D. S., Alzayady, K. J., Gygi, S. P., and Wojcikiewicz, R. J. H. (2008) *J. Biol. Chem.* **283,** 35319–35328
34. Newton, K., Matsumoto, M. L., Wertz, I. E., Kirkpatrick, D. S., Lill, J. R., Tan, J., Dugger, D., Gordon, N., Sidhu, S. S., Fellouse, F. A., Komuves, L., French, D. M., Ferrando, R. E., Lam, C., Compaan, D., Yu, C., Bosanac, I., Hymowitz, S. G., Kelley, R. F., and Dixit, V. M. (2008) *Cell* **134,** 668–678
35. Peng, J., Schwartz, D., Elias, J. E., Thoreen, C. C., Cheng, D., Marsischky, G., Roelofs, J., Finley, D., and Gygi, S. P. (2003) *Nat. Biotechnol.* **21,** 921–926
36. Maes, K., Missiaen, L., Parys, J. B., De Smet, P., Sienaert, I., Waelkens, E., Callewaert, G., and De Smedt, H. (2001) *J. Biol. Chem.* **276,** 3492–3497
37. Yoshikawa, F., Iwasaki, H., Michikawa, T., Furuichi, T., and Mikoshiba, K. (1999) *J. Biol. Chem.* **274,** 316–327
38. Soulsby, M. D., and Wojcikiewicz, R. J. H. (2005) *Biochem. J.* **392,** 493–497
39. Betzenhauser, M. J., Fike, J. L., Wagner, L. E., 2nd, and Yule, D. I. (2009) *J. Biol. Chem.* **284,** 25116–25125
40. Yule, D. I., Betzenhauser, M. J., and Joseph, S. K. (2010) *Cell Calcium* **47,** 469–479
41. Serysheva, I. I., Bare, D. J., Ludtke, S. J., Kettlun, C. S., Chiu, W., and Mignery, G. A. (2003) *J. Biol. Chem.* **278,** 21319–21322
42. Taylor, C. W., da Fonseca, P. C., and Morris, E. P. (2004) *Trends Biochem. Sci.* **29,** 210–219
43. Boname, J. M., Thomas, M., Stagg, H. R., Xu, P., Peng, J., and Lehner, P. J. (2010) *Traffic* **11,** 210–220
44. Goto, E., Yamanaka, Y., Ishikawa, A., Aoki-Kawasumi, M., Mito-Yoshida, M., Ohmura-Hoshino, M., Matsuki, Y., Kajikawa, M., Hirano, H., and Ishido, S. (2010) *J. Biol. Chem.* **285,** 35311–35319
45. Ye, Y., and Rape, M. (2009) *Nat. Rev. Mol. Cell Biol.* **10,** 755–764
46. Hofmann, R. M., and Pickart, C. M. (1999) *Cell* **96,** 645–653
47. Hassink, G., Kikkert, M., van Voorden, S., Lee, S. J., Spaapen, R., van Laar, T., Coleman, C. S., Bartee, E., Früh, K., Chau, V., and Wiertz, E. (2005) *Biochem. J.* **388,** 647–655
48. Li, W., Tu, D., Brunger, A. T., and Ye, Y. (2007) *Nature* **446,** 333–337
49. Dikic, I., Wakatsuki, S., and Walters, K. J. (2009) *Nat. Rev. Mol. Cell Biol.* **10,** 659–671
50. Sobhian, B., Shao, G., Lilli, D. R., Culhane, A. C., Moreau, L. A., Xia, B., Livingston, D. M., and Greenberg, R. A. (2007) *Science* **316,** 1198–1202
51. Wang, B., Matsuoka, S., Ballif, B. A., Zhang, D., Smogorzewska, A., Gygi, S. P., and Elledge, S. J. (2007) *Science* **316,** 1194–1198
52. Crosas, B., Hanna, J., Kirkpatrick, D. S., Zhang, D. P., Tone, Y., Hathaway, N. A., Buecker, C., Leggett, D. S., Schmidt, M., King, R. W., Gygi, S. P., and Finley, D. (2006) *Cell* **127,** 1401–1413
53. Rumpf, S., and Jentsch, S. (2006) *Mol. Cell* **21,** 261–269
54. Wertz, I. E., O'Rourke, K. M., Zhou, H., Eby, M., Aravind, L., Seshagiri, S., Wu, P., Wiesmann, C., Baker, R., Boone, D. L., Ma, A., Koonin, E. V., and Dixit, V. M. (2004) *Nature* **430,** 694–699
55. Marx, C., Held, J. M., Gibson, B. W., and Benz, C. C. (2010) *Cancer Res.* **70,** 3709–3717